

COMPARISON OF EMITTANCES AT 100, 200, 300, 400 GEV
IN THE PROTON EAST LINE

J. Hawkins

December 22, 1977

1. This report is a sequel to TM723 which relates the horizontal emittance ϵ_x at beam energies of 100, 200, and 400 GeV in the Proton East Pretarget Area. The major additions of this report are inclusive of FWHM values at 300 GeV and calculations of both ϵ_x and ϵ_y , horizontal and vertical emittances respectively. The results of this new data are summarized in Figures 1 and 2, and Table #6, which when translated into words allows the following statements:

a) ϵ_x in the given energy region is inversely proportional to beam energy:

$$\epsilon_x \approx \frac{1}{E}$$

b) ϵ_y in the given energy region is inversely proportional to beam energy:

$$\epsilon_y \approx \frac{1}{E}$$

c) The septum in Enclosure E clearly masks any vertical waist when a significant fraction (i.e. >20%) of beam is split.

2. Items a and b are easily understood from the respective figures, but "septum masking" requires a further explanation. To first order one can presume that the Proton beam line between SC311 and SC400 is a drift space with respect to the beam envelope. The 200 and 400 GeV envelope (i.e. practically no splitting) shows a vertical waist about 450 feet downstream of SC311. This distance is simply calculated from the transport¹ equation

$$L_{\text{waist}} = \frac{\sigma_{43}(0)}{\sigma_{44}(0)} = \frac{\alpha_y}{\gamma_y} \tag{1}$$

3. When beam split (i.e. moved vertically across the E septum) the vertical waist in the beam envelope disappears. Now, if one accepts the previous "drift space" assertion then it is reasonable to state that the E septum "masks" an otherwise existant waist. This effect can be seen in the 100 and 300 GeV data (i.e. Tables #5 and 3 respectively).

The factors contributing to this masking are twofold:

- a) Splitting the beam by the E septum reduces the vertical FWHM at SC311 by a factor directly proportional to the amount of split beam.² Thus a virtual waist is created at the septum location (i.e. SC311). However, the following 1st order transport¹ equation

$$(Y_1^2)_{\text{Max}} = (Y_0^2)_{\text{Max}} + L^2 (\theta_0^2)_{\text{Max}} \quad (2)$$

indicates that as L increases (i.e. as one moves downstream of SC311) the effect of changing $(Y_0)_{\text{Max}}$ via splitting is decreased. Consequently, when one includes the finite resolution of SWIC's (i.e. $\Delta\text{FWHM} = \pm 1\text{mm}$), the FWHM as seen at the waist, e.g. $L = 450$ feet, may not show any change when significant splitting occurs.

- b) Coulomb scattering of the Proton beam by the septum wires causes an increase in the beam phase space. This process is reflected by an increase of the FWHM at all positions downstream of the septum. The magnitude of this increase is 1% or 2%.² Inspection of equation #2 shows that this added angular divergence (i.e. $(\theta_0)_{\text{Max}}$) does contribute to the "masking" effect but to a lesser degree than changes in $(Y_0)_{\text{Max}}$.

4. As mentioned previously the "masking" phenomenon manifests itself in the 100 and 300 GeV data by reducing the ratio R,

$$R \equiv \frac{\text{SC311 (FWHM-V)}}{\text{SC319 (FWHM-V)}}$$

Thus in an attempt to compensate for this effect the vertical FWHM at SC311 has been increased by a factor directly proportional to the amount of beam split (See "comments" column in Tables 3 and 5).

5. Data and beam conditions used in this report are summarized in Tables 1,2,3, 4, and 5. The FWHM values are measured by hand. Emittances are determined via a program which includes error propagation. The quadratic coefficients are then related to α , β , γ , ϵ , the symbols used in the Courant and Snyder³ beam matrix formalism. See TM723 for more thorough statements concerning data acquisition, analysis, and boundary conditions.
6. A comparison of ϵ_x and ϵ_y in the P-East with those in P-Center can be found in Table #7. The FWHM values in this table were obtained by first splitting

all the Proton beam to P-Center, recording the beam profiles via photos, then switching all the beam to P-East and repeating the picture taking process. These results indicate the beam emittance is smaller in P-Center than in P-East.

7. ϵ_x in the Transfer Hall was approximately equal to 0.10 mm-mr^4 during the 400 GeV data taking. Consequently one sees, from Tables 6 and 7 that the 400 GeV horizontal emittance in the Proton East or Center Target Area is a factor of 3 larger than that in Transfer Hall. This growth in ϵ_x is understood in terms of non-conservative properties in the beam transport system. Properties such as time dependent magnetic fields during slow spill (i.e. ripple) and coulomb scattering of protons by SWIC's, septa, vacuum windows, etc., in the beam line.
 - 1) Transport/360, SLAC Report #91, Appendix 39-42.
 - 2) NAL Beam Splitting System
L. W. Oleniuk, R. A. Andrews, H. J. Bleser, C. H. Rode.
 - 3) E. D. Courant and H. S. Snyder, "Theory of the Alternating Gradient Synchrotron", Annals of Physics 3, Pages 1 through 48 (1958).
 - 4) H. Edwards and T. Murphy, Switchyard Studies at FNAL, (1976).

HORIZONTAL EMITTANCE
VS.
BEAM ENERGY

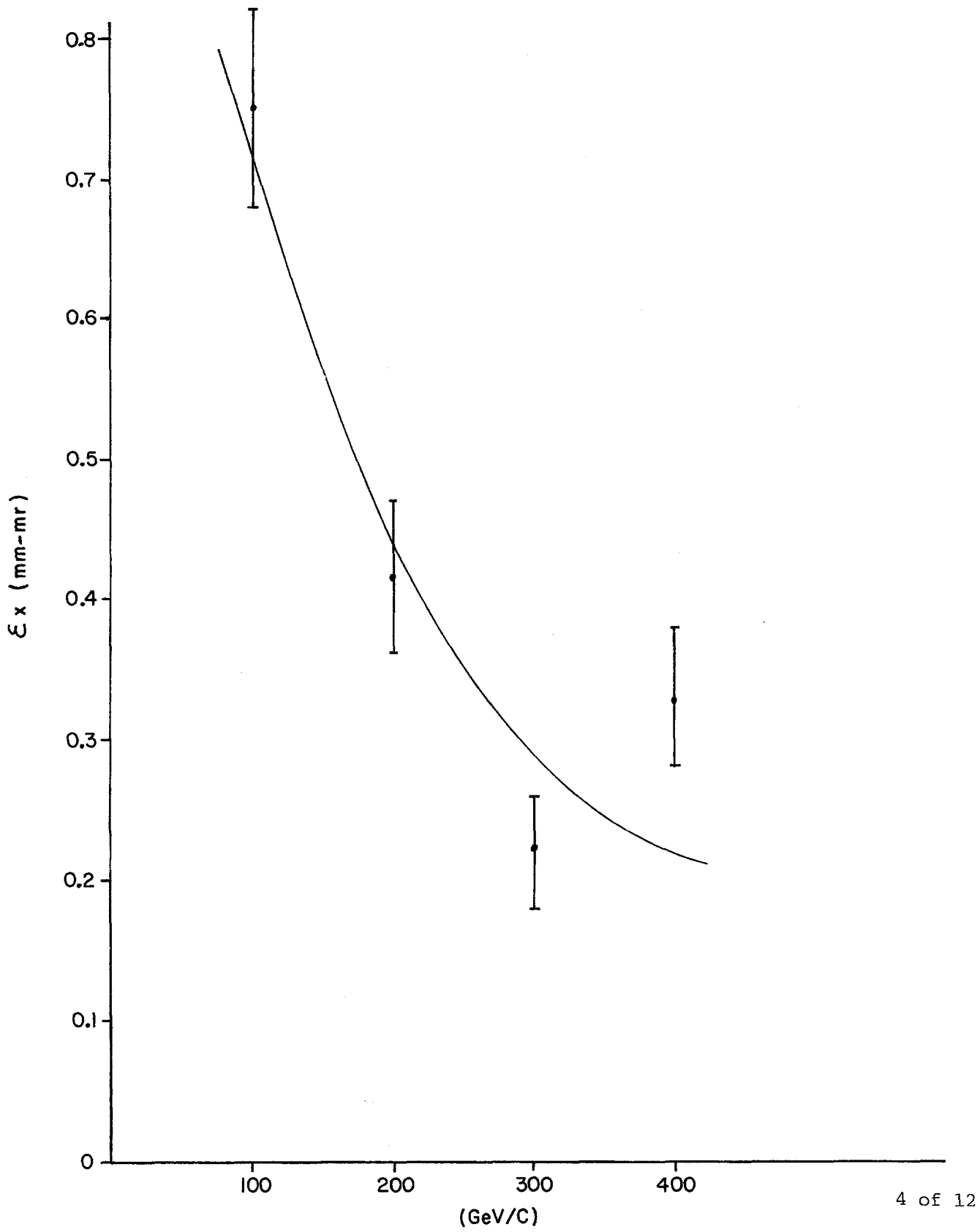
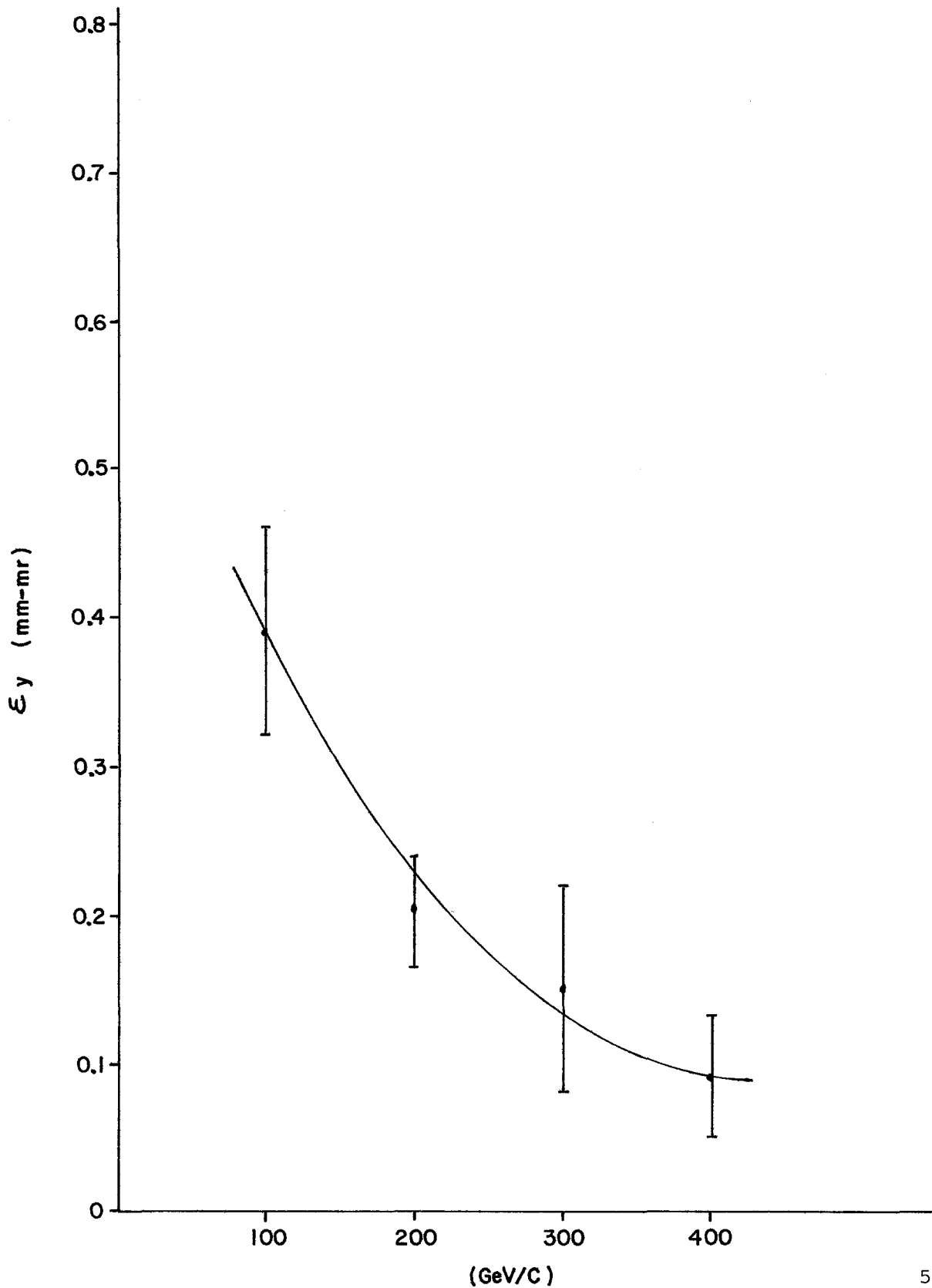


FIGURE 1

VERTICAL EMITTANCE
VS.
BEAM ENERGY



(GeV/c)
FIGURE 2

BEAM SPLIT CONDITIONS

<u>100 GeV</u>		<u>(9/19/76)</u>
P-West	3.0E10	
P-Center	1.0E10	
P-East	5.0E10	
Meson	\emptyset	
N- \emptyset	\emptyset	

<u>200 GeV</u>		<u>(9/19/76)</u>
M. R.	1.7E13	
P-West	5.0E10	
P-Center	1.0E10	
P-East	4.8E12	
N- \emptyset (East)	5.0E12	
N- \emptyset (Slow)	2.0E12	
N-7	3.0E10	
Meson	2.5E12	

<u>400 GeV</u>		<u>(11/11/76)</u>
M. R.	1.7E13	
P-West	2.0E10	
P-Center	1.0E10	
P-East	3.0E12	
N- \emptyset (Fast)	\emptyset	
N- \emptyset (Slow)	1.1E13	
N-7	2.0E11	
Meson	2.4E12	

<u>300 GeV</u>		<u>(9/27/77)</u>
M. R.	8.2E12	
P-East	9.5E10	
P-West	4.7E10	
N- \emptyset (Slow)	1.2E11	
N-7	1.0E11	
Meson	7.3E12	

DEVICE	FWHM-V (mm)	DATE	COMMENTS	FWHM-H (mm)	DATE	COMMENTS
SCMQ300	4.0 5.0 4.0 4.3 ± .5mm	10/22(0055) 10/26(0230) 11/11(0400)		8.0 1.0 1.1 1.0 ± .5	10/23(0055) 10/11(0400) 11/11(0400)	H.G.
SCMQ302	? ? 3.0 2.0 ± .5mm			11.0 8.2 6.8 7.0 ± .5		H.G. OFF H.G. OFF
SCMQ302	5.0 5.0 4.0 4.7 ± .5mm			3.0 4.0 4.0 3.3 ± .5		
SCMQ305	3.0 5.0 2.0 2.7 ± .5mm			6.0 6.0 8.0 7.0 ± .5		
SCMR400	3.0 3.0 3.0 3.0 ± .5mm			16.0 16.0 16.0 16.0 ± .5		
SCMQ310	5.0 5.0 6.0 5.3 ± .5mm			20.0 20.0 48.0 20.0 ± .5		
SCESEP E	7.0 7.0 8.0 ± 1mm			15.0 15.0 16.0 15.3 ± .5		
SCMV310E	4.0 3.0 4.0 3.0 ± 1mm			13.0 14.0 17.0 15.0 ± .5		
SC319/320	7.0 ± 1 6.5 ± 1	10/23 11/20(1730) 11/20	319E 320E	13.0 ± 2 10.0 ± 2	11/30(1730) 11/20(1730)	319E 320E
SC323	6.0 ± 1	11/20(1730)		1.1 ± .5	11/20(1730)	
SC400	14.0 ± 2	11/20		22.0 ± 2mm	11/20	

TABLE #2

300 GeV

DEVICE	FWHM-V (mm)	DATE	COMMENTS	FWHM-H (mm)	DATE	COMMENTS
SCMQ300	5.0	9/27/77		9.0	9/27/77	
SCMQ302	3.0	9/27/77		9.0	9/27/77	
SCMQ303	5.0	9/27/77		8.0	9/27/77	
SCMQ305	3.0	9/27/77		7.0	9/27/77	
SCMH400	5.0	9/27/77		9.0	9/27/77	
SCMQ310	6.0	9/27/77		11.0	9/27/77	
SCESEP	6.0±2.0 ≈9.0±2.0	9/27/77	D.S. of 1st Split Add. Fraction α Split Ratio (1.5)	11.0 ±1.0	9/27/77	
SCMV310E	5.0 ±1mm	9/27/77		8.5mm ±.5mm	9/27/77	
SC319E	3.5W =10.0±2mm	9/27/77		2.5W =8.5mm±2mm	9/27/77	
SC320E	3.0W 9.0±2mm	9/27/77		3.0 10.0±2mm	9/27/77	
SC232E	8W =8mm±1mm	9/27/77		8.5W =8.5±1mm	9/27/77	
SC400	9W=18mm	9/27/77		14W=28mm	9/27/77	

TABLE #3

DEVICE	FWHM-V (mm)	DATE	COMMENTS	FWHM (mm)	DATE	COMMENTS
SCMQ300	5.0	9/19(1800)		6.0	9/19(1800)	
	6.0	9/19(1100)		2.0	9/19(1100)	
	6.0	9/17(1000)		2.0	9/17(1000)	
AVERAGE	5.7±.5			3.3±.5		
SCMQ302	2.0	9/19		8.0	9/19	
	4.0	9/19				
	4.0	9/17		8.0	9/17	
AVERAGE	3.5±.5			8.0±.5		
SCMQ303	6.0	9/19		4.0	9/19	
	4.0	9/19		4.0	9/19	
	4.0	9/17		4.0	9/17	
AVERAGE	4.7			4.0±.5		
SCMQ305	5.0	9/19		6.0	9/19	
	5.0	9/19		6.0	9/19	
	5.0	9/17		6.0	9/17	
AVERAGE	5.0±.5			6.0±.5		
SCMH300	7.0	9/19		13.0	9/19	
	7.0	9/19		13.0	9/19	
	7.0	9/17		14.0	9/17	
AVERAGE	7.0±.5			13.3±.5		
SCMQ300	5.0	9/19		19.0	9/19	
	9.0	9/19		19.0	9/19	
	8.0	9/17		19.0	9/17	
AVERAGE	7.3±.5			18.3±.5		
SCSEEP	7.0	9/19		12.0	9/19	
	11.0	9/19		14.0	9/19	
	10.0	9/17		13.0	9/17	
AVERAGE	9.3±.5			13.0±.5		
SCMV310E	6.0	9/19		12.0	9/19	
	6.0	9/19		13.0	9/19	
	6.0	9/17		13.0	9/17	
AVERAGE	6.0			12.9		
SC319/320	9.0±5mm	9/19(1800)		10.0±3mm	9/19	
SC323	10.0±1mm	9/19(1800)		10.0±1mm	9/19	
SC400	22.0±2mm	9/19(1800)		36.0±2mm	9/19	

TABLE #4

100 GeV

DEVICE	FWHM-V (mm)	COMMENTS	FWHM-H (mm)	COMMENTS
SCMQ300	6.0±.5	9/19(1800)	13.0±.5	19/19(1800)
SCMQ302	3.0±.5		11.0±.5	
SCMQ303	9.0±.5		7.0±.5	
SCMQ505	8.0±.5		10.0±.5	
SCMQ400	6.0±.5		21.0±.5	
SCMQ310	8.0±.5		35.0±.5	
SCSEEP	9.0±.5	9.0→10.5 via Masking Factor	20.0±.5	
SEMV310E	8.0±.5		21.0±.5	
SC319/320E	15.0±.5		15.0±1.0	
SC323	15.0±1.0		15.0±1.0	
SC400	30.0±2.0		40.0±2.0	

TABLE #5

σ MATRIX PARAMETERS

	100 (GEV)	200 (GEV)	300 (GEV)	400 (GEV)	COMMENTS
ϵ_x (mm-mr.)	0.752	0.414	0.223	0.327	
ϵ_y (mm-mr.)	*	0.204	*	0.095	*≡ Masking factors Included
α_x	0.883	0.925	0.685	0.578	
α_y	0.206	0.429	0.145	0.286	
β_x	531.6	407.9	323.8	687.6	
β_y	466.0	423.9	538.5	514.1	
γ_x	.003	0.004	0.004	0.002	
γ_y	0.002	0.003	0.002	0.002	
L_x (feet)	956.5	751.5	556.5	939.2	
L_y (feet)	*	464.7	*	464.7	*3 Masking Factors Included

TABLE #6

σ MATRIX PARAMETERS

	6/7/75		4/5/75		COMMENTS
	ALL PC	ALL PE	ALL PC	ALL PE	
ϵ_x (mm-mr)	.33±.03	.44±.04	.244±.08	.402±.05	
ϵ_y (mm-mr)	.10±.02	.11±.02	.120±.02	.127±.03	6/7/75: Average ppp = 2E12
α_x	.678	.407	.010	.77	
α_y	.332	.451	.599	.61	4/5/75: Average ppp = 7E10
β_x	673.2	473.7	540.9	327.5	
β_y	342.4	261.0	351.8	331.7	
γ_x	.002	.002	.002	.004	
γ_y	.003	.004	.004	.004	
L_x (feet)	1001	661	25	625	
L_y (feet)	360	366	487	496	

TABLE #7